$\mathcal{PT}$ symmetric models in more dimensions and solvable square-well versions of their angular Schrödinger equations

2003 J. Phys. A: Math. Gen. 36 7825

(http://iopscience.iop.org/0305-4470/36/28/311)

INSTITUTE OF PHYSICS PUBLISHING JOURNAL OF PHYSICS A: MATHEMATICAL AND GENERAL

J. Phys. A: Math. Gen. **36** (2003) 7825–7838 PII: S0305-4470(03)61885-8

$\mathcal{PT}$ symmetric models in more dimensions and solvable square-well versions of their angular Schrödinger equations

Miloslav Znojil

Ústav jaderné fyziky AV ČR, 250 68 Řež, Czech Republic

E-mail: znojil@ujf.cas.cz

Received 7 April 2003, in final form 20 May 2003
Published 1 July 2003
Online at stacks.iop.org/JPhysA/36/7825

Abstract

From the partial differential Calogero's (three-body) and Smorodinsky–Winternitz (superintegrable) Hamiltonians in two variables we separate the respective angular Schrödinger equations and study the possibilities of their 'minimal' $\mathcal{PT}$ symmetric complexification. The simultaneous loss of the Hermiticity and solvability of the respective angular potentials $V(\varphi)$ is compensated by their replacement by solvable, purely imaginary and piecewise constant multiple wells $V_0(\varphi)$. We demonstrate that the spectrum remains real and that it exhibits a rich 'four series' structure in the double-well case.

PACS number: 03.65.Fd

1. Introduction

One of the most important methods of solution of partial differential Schrödinger equations in D dimensions is an approximate [1] or exact [2] separation of variables in spherical coordinates. For example, once the potential is central, $V(\vec{r}) = V(|\vec{r}|)$, the angular part of each wavefunction coincides with the well-known D dimensional (hyper)spherical harmonics.

In the non-central case the explicit examples range from the confinement of a single (quasi-)particle in a superintegrable Smorodinsky–Winternitz potential [3] up to the binding of $A > 1$ particles in the exactly solvable models of the Calogero–Moser–Sutherland type [4, 5]. Of course, the structure of the corresponding D dimensional generalizations of the (hyper)spherical harmonics becomes more complicated. Our present study was inspired precisely by this problem.

In section 2 we shall introduce some basic notions and a few explicit more or less standard examples of the above-mentioned partial differential Schrödinger equations (cf subsection 2.1 for more details). Then we shall specify our main purpose, namely, the analysis of the models in question in their appropriate non-Hermitian generalizations (a few remarks about motivation will be collected in subsection 2.2). In such a setting, subsection 2.3 will summarize the key technical aspects of our project.

In section 3 we shall specify and explain in some detail the present implementation of the Bender and Boettcher idea [6] of weakening the traditional Hermiticity to mere $\mathcal{PT}$ symmetry. Subsection 3.1 will show that once we decided to study just the two-dimensional partial differential Schrödinger equations, their angular part degenerates to the mere single ordinary differential equation,

$$\left[-\frac{\mathrm{d}^2}{\mathrm{d}\varphi^2}+V(\varphi)\right]\psi(\varphi)=\ell^2\psi(\varphi) \qquad \varphi\in(0,2\pi). \tag{1}$$

This simplifies many technical aspects of our problem which may be re-formulated as a confinement of a quasi-particle on a circle [7]. Unfortunately, in contrast to the standard models which use the Hermitian Hamiltonians and in which both the interpretation and the solution of the angular Schrödinger equation (1) remain straightforward, we encounter a really serious difficulty here since the weakening of the Hermiticity makes our potentials $V(\varphi)$ unsolvable. As we shall show below, they all acquire a multi-well shape with some $2M$ high barriers and deep minima all over the circle.

Recently we $\mathcal{PT}$ symmetrized the three-body Calogero model only via a very specific complexification of its angular part (1) which enabled us to find new solutions and to write them all down in closed form [8]. This admitted a preservation of many parallels between the Hermitian and non-Hermitian case. Still, one cannot assert that our recipe was fully satisfactory since, first of all, we did not provide any guarantee that the construction of the solutions in polynomial form gives us all the existing solutions. For this and other reasons we are going to suggest now an alternative $\mathcal{PT}$ symmetrization recipe.

The details will be described in subsection 3.2 where we postulate that all our angular potentials possess just a suitable *piece-wise constant* shape which is, in addition, *purely imaginary*. In this way, our choice will parallel many popular and purely imaginary $\mathcal{PT}$ symmetric models on the real line. *Simultaneously*, we merely lose a small part of the simplicity of the central models where the angular Schrödinger equation may be re-interpreted as a square well in quantum mechanics on a circle. For a more detailed explanation of such a point of view, cf the first paragraph in subsection 2.1.

By construction, our multiple imaginary square wells on a circle remain solvable by the matching method in principle. In practice, this is illustrated in section 4 where we contemplate the simplest non-trivial two-dimensional problems of the above-mentioned partial differential form. In technical terms, this section deals with the angular Schrödinger equation defined on a circle and is the core of our present work. Subsection 4.1 describes some details concerning the implementation of the current matching method, and subsection 4.2 offers an ample illustration of this recipe and its results. In the three tables we sample the resulting spectra and discuss their apparent split into four sub-series. Some methodical aspects of the practical search for these energies are clarified with the assistance of several figures. They document the reliability of the method and show that just keeping in mind a few simple rules concerning the (numerical) scaling, one may calculate the energies with *any* pre-determined precision.

In section 5 we place all our results in a broader context, i.e. of the popular double-well problems in subsection 5.1 and of their specific 'angular' features in subsection 5.2.

2. Angular Schrödinger equations

2.1. Hermitian non-central models

Let us recollect the simplest possible two-dimensional situation where the angular Schrödinger equation (1) is just one dimensional and defined on a circle (i.e. with the periodic boundary conditions). In all the central cases it contains just the trivial potential term, $V(\varphi) = 0$ for all $\varphi \in (0, 2\pi)$. Hence, the well-known (hyper)spherical solution of equation (1) is immediate, $\psi_m(\varphi) = \exp \mathrm{i}m\varphi$, $\ell \equiv m = 0, 1, \ldots$.

In all the less trivial but still fully separable and exactly solvable models with non-central potentials, the angular Schrödinger equation (1) remains exactly solvable by assumption. One may recollect one of the oldest and simplest illustrative examples of this type, namely, the Smorodinsky–Winternitz 'superintegrable' oscillator in two dimensions [3],

$$\left[-\frac{\partial^2}{\partial X^2} - \frac{\partial^2}{\partial Y^2} + X^2 + Y^2 + \frac{G}{X^2} + \frac{G}{Y^2}\right]\Phi(X, Y) = \mathcal{E}\Phi(X, Y). \tag{2}$$

After a routine elimination of the uninteresting motion of the centre of mass, the partial differential representation of Calogero's popular three-body bound-state model [4] also has a very similar form

$$\left[-\frac{\partial^2}{\partial X^2} - \frac{\partial^2}{\partial Y^2} + X^2 + Y^2 + \frac{g}{2X^2} + \frac{g}{2(X - \sqrt{3}Y)^2} + \frac{g}{2(X + \sqrt{3}Y)^2}\right]\Phi(X, Y) = \mathcal{E}\Phi(X, Y). \tag{3}$$

Due to the presence of the repulsive barriers at $G > 0$ and $g > 0$, the angular parts of both these equations cease to be defined on the corresponding hypersphere (i.e. on the circle). Thus, once we distinguish the above two models by their respective 'label numbers' $M = M_{\text{Winternitz}} = 2$ and $M = M_{\text{Calogero}} = 3$, we may summarize that

(a) the domain of our innovated harmonics $\psi(\varphi)$ (sometimes called the Weyl chamber) shrinks to a segment $\varphi \in (0, \pi/M)$ of the full circle,
(b) at both the ends of this interval, the Dirichlet boundary conditions must be imposed, due to the presence of a strong singularity there,
(c) both the models (with the elementary Pöschl–Teller angular potentials) still remain exactly solvable, as expected, in terms of Jacobi polynomials [9].

All three comments (a)–(c) remain valid also for an oversimplified 'toy' model

$$\left[-\frac{\partial^2}{\partial X^2} - \frac{\partial^2}{\partial Y^2} + X^2 + Y^2 + \frac{\mathcal{G}}{X^2}\right]\Phi(X, Y) = \mathcal{E}\Phi(X, Y). \tag{4}$$

Its 'index' $M = M_{\text{toy}} = 1$ is 'minimal' and the model is popular as a not entirely trivial methodical guide [4, 8]. It will play the same guiding role in what follows.

2.2. A motivation for transition to non-Hermitian Hamiltonians

In the recent literature, increasing attention is being paid to non-Hermitian Hamiltonians with real spectra. Mostly they are characterized by their parity-times-time-reversal symmetry, $H = \mathcal{PT}H\mathcal{PT}$ [6, 9, 10] or, in a more formal setting, by their specific parity-pseudo-Hermiticity property $H = \mathcal{P}H^\dagger\mathcal{P}$ [11–13]. Via analytic continuation this tendency seems to offer a non-trivial insight into the solutions [14].

An important *phenomenological* appeal of similar studies is related to the observation that the complex conjugation operator $\mathcal{T}$ mimics the time reversal [15, 16]. The early stages of

development of this subject were co-motivated by its natural emergence within perturbation studies of various models in quantum mechanics and field theory. People revealed, for example, that even the peculiar and 'strongly non-Hermitian' imaginary cubic anharmonic oscillator may have a real and discrete spectrum bounded from below [17, 18]. A few years later, the introduction of an 'unstable' quartic anharmonic oscillator proved *mathematically* relevant in having facilitated the perturbative description of some apparently non-perturbative double-well models (e.g. $H^{(DW)}(g) = p^2 + x^2(1 - gx^2)^2 + cx$ in [12]). The weakening of the Hermiticity to mere pseudo-Hermiticity was even found to make the non-Hermitian quartic oscillators exactly solvable at certain couplings and energies [19].

The quick progress in the field has led to the sophisticated perturbative analyses of some non-Hermitian $\mathcal{PT}$ symmetric models in more dimensions [20]. The 'analytic continuation' activities intensify since the Hermitian non-central partial differential Schrödinger equations are attractive by the variability of their possible *physical* interpretations. They might prove relevant in the models which range from a single particle moving in a non-central D dimensional potential [21] up to a full-fledged A body motion and spectra [22]. Still, the real impact of their non-Hermitian analytic continuations is not yet fully predictable at present.

In contrast to the majority of contemporary publications which study the $\mathcal{PT}$ symmetric models in one dimension, one also has no clear guide to the purely technical aspects of the $\mathcal{PT}$ symmetrization of the models in more dimensions. We feel motivated by this mathematical challenge and intend to pay deeper attention to the specific subset of the $\mathcal{PT}$ symmetrization techniques which is based on an 'incomplete' complexification involving just the 'angular' part of the problem.

Without any detour to perturbation methods we shall study some specific properties of a class of the 'angular' Schrödinger equations in a way encouraged by our experience with the comparatively easy tractability and insight provided by the piece-wise constant potentials [23].

2.3. Complexifications of the angular Schrödinger equations

Within the framework of the so-called $\mathcal{PT}$ symmetric quantum mechanics [16] one may complexify the model (3) of Calogero [8, 24] as well as its spiked and superintegrable predecessors (2) [25] by the complexification of its single angular coordinate. Such an approach remains sufficiently transparent. One of its very friendly features is that it leads to a perceivable strengthening of the analogies between many of the above-mentioned non-central models (with $g \neq 0$ in equation (3) or with $G \neq 0$ in equation (2)) and their central, regular special cases (with $g = 0$ or $G = 0$, respectively).

In what follows, we just intend to study these analogies in more detail. In a more explicit formulation of this purpose, our analysis will start from the weakening of the Hermiticity to the mere $\mathcal{PT}$ symmetry of the Hamiltonian. This opens a way towards a suitable complex deformation of the integration path [6], especially in the vicinity of the singular points $\varphi_k = \pi k/M, k = 1, 2, \ldots, 2M$. In this sense one should

(a) re-extend the domain of the complexified harmonics $\psi(\varphi)$ to the full circle,
(b) return to the standard periodic boundary conditions in order to keep our wavefunctions unambiguously defined,
(c) re-analyse the solutions of equation (1) in the complex domain.

Unfortunately, none of the existing papers solved all three problems (a)–(c) at once. In particular, [26] studied the solutions of equation (1) on a single, isolated complex segment, while a return to the full circle has been facilitated in [8, 25] by the use of the 'non-periodic', Dirichlet boundary conditions.

An incompleteness of the latter results formed a key inspiration of our present paper. In essence, it will circumvent some of the main technical obstacles via a simple-minded replacement of the complexified Pöschl–Teller potentials in equation (1) by their square-well-like solvable approximants.

3. Toy models on a circle

3.1. A constant complex shift of the angle φ

Let us consider one of the above-listed angular Schrödinger equations (1) with the Pöschl–Teller M-dependent potential. One of its simplest complexifications on a circular domain will be then determined by a mere constant complex shift (plus a comfortable re-scaling) of the angular variable,

$$\varphi = \varphi(s) = -\mathrm{i}\alpha + \frac{\pi}{2}s \qquad \alpha > 0 \qquad s \in (-2, 2). \tag{5}$$

Whenever the imaginary shift is very large, $\alpha \gg 1$, the Pöschl–Teller potential itself becomes very smooth and 'almost forgets' about all its singularities along the real line,

$$V^{(\mathrm{PT})}(\varphi) \sim 1/\sin^2(M\varphi) = \mathrm{e}^{-2M\alpha} \cdot [-\cos \pi M s + \mathrm{i} \sin \pi M s + \mathcal{O}(\mathrm{e}^{-2M\alpha})]. \tag{6}$$

This potential is non-Hermitian and manifestly $\mathcal{PT}$ symmetric (with the current definition of the complex conjugation $\mathcal{T}$ and parity $\mathcal{P}s = -s$). In the generic case, its 'energies' (or rather eigenvalues ℓ^2 in equation (1)) may be expected to be real [16]. In addition, its wavefunctions may be comfortably expressed in terms of Bessel functions [27].

Unfortunately, the above solutions only become exact in the limit $\alpha \to \infty$ where the potential (6) itself vanishes. Obviously, all the information about the original angular potential is lost and nothing new is gained in the limit $\alpha \to \infty$ since, formally, one just returns to hyperspherical harmonics. Conversely, trying to preserve the specific, $2M$-well character of our family of the Pöschl–Teller angular potentials $V^{(\mathrm{PT})}$ *we must return* to the domain of the finite shifts α. In what follows, we intend to take just the first steps in this direction.

3.2. Piece-wise constant angular potentials

Basically, we shall preserve the multi-well character of our potentials, trying merely to deform the local details of their global shape. In a more detailed specification of our 'toy-model' we were guided by [28] and [29]. In the former, the complex and $\mathcal{PT}$-symmetric potentials with elementary trigonometric shapes resembling equation (6) have been analysed in the *periodic* case. In accordance with expectations, the corresponding band spectrum proved real but in contrast to the conventional real periodic potentials, it appeared to exhibit certain significant *qualitatively new* features. Although, due to the unsolvable character of the potentials, all these observations were originally based just on the careful numerical analysis and higher-order WKB techniques, their confirmation has been delivered in the subsequent short note [29]. There, the presumably not too relevant real part of the 'realistic' potential V has been replaced by a constant (zero). Moreover, the exact solvability of the new schematic model has been achieved by an extremely drastic reduction of all the remaining (i.e. purely imaginary) part of the potential V to the mere sequence of delta functions (known as the Kronig–Penney model) with purely imaginary (i.e. still $\mathcal{PT}$-symmetric) strengths mimicking the presence of the infinitely many minima in the original V.

Here we shall proceed in a very similar manner. Firstly, we shall ignore again the real part of the potential as not too relevant. Besides all the above-mentioned indirect motivation

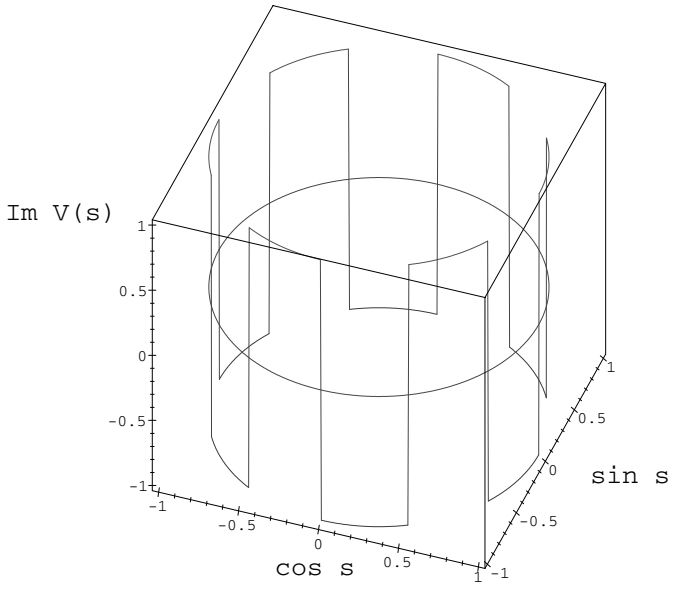

Figure 1. Imaginary part of a Calogerian six-well angular potential in its rectangular approximation.

of such a technical simplification, we also directly verified its consistency in [30] where a 'minimal' *non-periodic* double-well version of the Kroning–Penney potential has been used.

Secondly, we shall keep in mind that the most important feature of the remaining, purely imaginary part of our potentials (6) lies in the presence of their *precisely* $2M$ separate extremes. Thus, a transition to the solvable model will be achieved here via their *piece-wise constant* approximation. In this manner, once we denote $h = 1/M$, we arrive at the angular Schrödinger equation (1) in the more or less unique form

$$\left[-\frac{\mathrm{d}^2}{\mathrm{d}s^2} + V^{(M)}(s)\right]\psi^{(M)}(s) = E\psi^{(M)}(s) \qquad s \in (-2, 2) \tag{7}$$

with the very specific class of the purely imaginary toy potentials

$$V^{(M)}(s) = \pm \mathrm{i}Z \qquad \text{for} \quad s \in \triangle^{(\pm)} \tag{8}$$

where

$$\triangle^{(+)} = (-2, -2+h)\bigcup(-2+2h, -2+3h)\bigcup\cdots\bigcup(2-2h, 2-h)$$

and

$$\triangle^{(-)} = (-2+h, -2+2h)\bigcup\cdots\bigcup(2-3h, 2-2h)\bigcup(2-h, 2).$$

For illustration, figure 1 shows the shape of such a potential defined over the circle at the Calogero choice of $M = 3$.

In what follows we shall consider our potentials (8) and concentrate on their first non-trivial special case with $M = 1$,

$$V(x) = \begin{cases} +\mathrm{i}Z & x \in (-2, -1)\bigcup(0, 1) \\ -\mathrm{i}Z & x \in (-1, 0)\bigcup(1, 2) \end{cases}. \tag{9}$$

This means that a combination of the $\mathcal{PT}$ symmetry requirement with the double-well character of the potential makes our $M = 1$ model defined on a circle of the convenient radius $R = 2/\pi$.

4. Solutions

4.1. The sample of the matching conditions at $M = 1$

The explicit solutions of our toy example (9) will be constructed by the matching method. For this purpose, it makes sense to denote the left and right intervals $(-2, 0)$ and $(0, 2)$ by the respective subscripts $_L$ and $_R$. The subintervals which lie near or far from the origin at $s = 0$ will be assigned another subscript $_N$ or $_F$, respectively. In this notation we have the natural ansatz

$$\psi_j(x) = A_j \sin \kappa_j x + B_j \cos \kappa_j x \qquad j = FL,\ NL,\ NR,\ FR \tag{10}$$

with

$$\kappa_{FL} = \kappa_{NR} = \kappa = s - \mathrm{i}t \qquad \kappa_{NL} = \kappa_{FR} = \kappa^* = s + \mathrm{i}t \qquad s > 0 \quad t > 0. \tag{11}$$

This should be interpreted as a mere suitable reparametrization of the desired spectrum of 'energies'

$$E \equiv \ell^2 = s^2 - t^2 \qquad 2st \equiv Z > 0. \tag{12}$$

Now it is easy to require the matching of the logarithmic derivatives at the discontinuity at $x = -1$,

$$\psi_{FL}(-1) = \psi_{NL}(-1) \qquad \psi'_{FL}(-1) = \psi'_{NL}(-1) \tag{13}$$

and, *mutatis mutandis*, at the other two 'internal' boundaries at $x = 0$ and $x = 1$. The points $x = 2$ and $x = -2$ must be matched together in a way which reflects the circular symmetry of the problem,

$$\psi_{FR}(2) = \psi_{FL}(-2) \qquad \psi'_{FR}(2) = \psi'_{FL}(-2). \tag{14}$$

We may conclude that the elementary insertions lead to the linear system of eight homogeneous equations for all the eight coefficients A_j and B_j (which may be arbitrarily normalized). This means that the secular determinant of the system must vanish,

$$\det Q(s, t) = 0. \tag{15}$$

After one inserts, say, $s = s(t) = Z/2t$ from equation (12), the insertion of all the non-vanishing matrix elements leads to the closed and compact form $F(t) = 0$ of equation (15) with

$$Q_{11} = -Q^*_{13} = -Q_{55} = Q^*_{57} = -\sin\kappa \tag{16}$$

$$Q_{12} = -Q^*_{14} = Q^*_{34} = -Q_{36} = Q_{56} = -Q^*_{58} = \cos\kappa \tag{17}$$

$$Q_{21} = -Q^*_{23} = Q^*_{43} = -Q_{45} = Q_{65} = -Q^*_{67} = \kappa\cos\kappa \tag{18}$$

$$Q_{22} = -Q^*_{24} = -Q_{66} = Q^*_{68} = \kappa\sin\kappa \tag{19}$$

$$Q_{71} = Q^*_{77} = -\sin 2\kappa \qquad Q_{72} = -Q^*_{78} = \cos 2\kappa \tag{20}$$

$$Q_{81} = -Q^*_{87} = \kappa\cos 2\kappa \qquad Q_{82} = Q^*_{88} = \kappa\sin 2\kappa \tag{21}$$

and

$$F(t) = -8t^4 \sinh^6 t \sin^6\left(\frac{1}{2t}\right) + \cdots - \frac{1}{2t^4}\cosh^6 t \cos^6\left(\frac{1}{2t}\right). \tag{22}$$

We did not display it here in full detail because with all its 30 separate real trigonometric terms, this explicit formula is quite lengthy and its detailed inspection seems hardly instructive at all. For this reason, we are rather going to display here a few characteristic graphs of the function $F(t)$ instead.

Table 1. The low-lying energy spectrum at $Z = 1$.

Level n	Parameter t_n	Energy E_n	Difference $\triangle_n$ $E_n - E_{n-1}$
0	0.656	0.149 312	–
1	0.393	1.459 965	1.319
2	0.266	3.464 686	2.004
3	0.159 6	9.792 771	6.328
4	0.158 7	9.895 111	0.102
5	0.111	20.127 356	10.232
6	0.101	24.273 237	4.146
7	0.079 59	39.459 389	15.186
8	0.079 56	39.484 770	0.025
9	0.065 1	58.954 565	19.469
10	0.062 3	64.410 749	5.456
11	0.053 053	88.817 991	24.397
12	0.053 050	88.829 258	0.011
13	0.046 1	117.648 14	28.819
14	0.044 9	124.154 74	6.507
15	0.039 789	157.908 92	33.754
16	0.039 788	157.915 26	0.006
17	0.035 7	196.154 02	38.239

Table 2. Two natural subsets of the even energy levels of table 1.

Level n	Second difference $\triangle_n - \triangle_{n-4}$	Level n	Second difference $\triangle_n - \triangle_{n-4}$
6	2.142	8	−0.77
10	1.310	12	−0.014
14	1.051	16	−0.0049

4.2. The sample of a graphical determination of the spectrum

One should start in a weak coupling regime. Choosing the very small $Z = 1/10$ we get the sequence $t_0 = 0.221\,981\,956\,2$, $t_1 = 0.034\,670\,670\,57, \ldots$ of the real roots of $F(t)$. Due to the fact that the function $F(t)$ itself has elementary form, the numerical values of these roots may easily and quickly be evaluated with arbitrary precision. These values then determine the low-lying energies $E_0 = 0.001\,532\,55$, $E_1 = 2.078\,577$ etc.

An increase of the coupling to $Z = 1$ shifts the lowest roots ($t_0 = 0.656\,419\,5696$ etc) and energies ($E_0 = 0.149\,312\,3386$ etc) upwards. No changes in the pattern are observed, and a more detailed description of the $Z = 1$ results is given in tables 1–3.

These sample results reveal and demonstrate a certain quadruple periodicity of the energy levels. This merely reflects the simplicity and regularity of the secular determinant $F(t)$ itself. An inspection of the overall shape of this function clarifies the structure of the spectrum in a way which complements the explicit tables very well. Thus, we may see in figure 2 that beyond its rightmost or 'maximal' root $t_0 \approx 0.66$, the curve $F(t)$ remains negative and decreases towards $-\infty$ very quickly.

In a way, the ground-state root t_0 has a certain 'exceptional' status in having no natural 'neighbour'. For the rest of the spectrum we observe that the roots may be organized as certain doublets (t_{2k-1}, t_{2k}) numbered by $k = 1, 2, \ldots$. With an increase of the index k, these partners

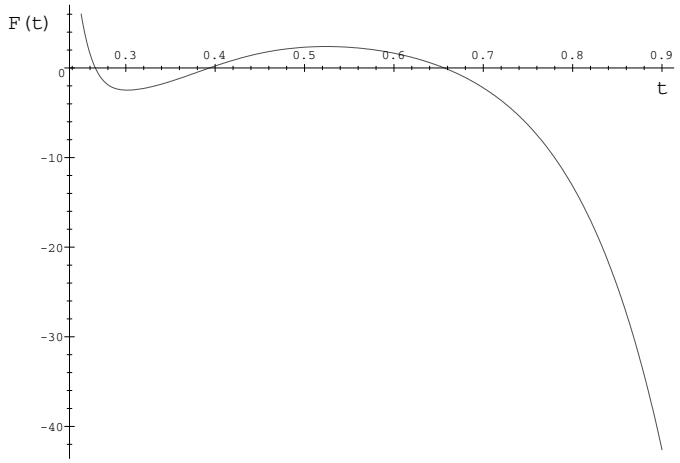

Figure 2. Monotonic decrease of the secular determinant $F(t)$ beyond its ground-state root $t_0 \approx 0.656$ at $Z = 1$.

Table 3. Two natural subsets of the odd energy levels of table 1.

Level n	Second difference $\triangle_n - \triangle_{n-2}$	Third difference $\triangle_n - 2\triangle_{n-4} + \triangle_{n-8}$
3	5.018	–
5	3.904	−1.114
7	4.954	+1.050
9	4.283	−0.671
11	4.938	+0.655
13	4.422	−0.516
15	4.935	+0.513
17	4.485	−0.450

in the doublet lie closer and closer to each other. This is illustrated in figure 3 where an onset of the existence of the doublets is clearly visible near $t_1 = 0.393\,471\,0177$ and where we also notice a rapid growth of the maxima of $F(t)$ which makes the numerical search for its zeros slightly more complicated. In particular, it is necessary to keep the necessary re-scalings of $F(t)$ during its graphical analysis under control.

For this purpose we used an algorithm based on an interplay between the plotting and root searching steps. For example, the doubts over figure 3 concerning the existence of the root near $t \approx 0.16$ are easily settled by the magnification of this subinterval in figure 4. In this way we were able to detect and scale-out the comparatively quick increase of the density of the roots $t_n > 0$ with the increase of their subscripts.

A new phenomenon emerged in the domain of $n \gg 1$, which may be noticed in figure 4. One detects a systematically growing difference between the behaviour of the doublets (t_{2k-1}, t_{2k}) at their even and odd indices k. The phenomenon is still more visible after we move to the energies themselves. Thus, a glimpse in table 1 verifies immediately that only at even $k = 2m$ does the quasi-degeneracy of the pairs of roots (t_{2k-1}, t_{2k}) have a real impact. Only in this case it implies also a similar quasi-degeneracy effect for the related energies, $E_{4m-1} \approx E_{4m}, m \gg 1$.

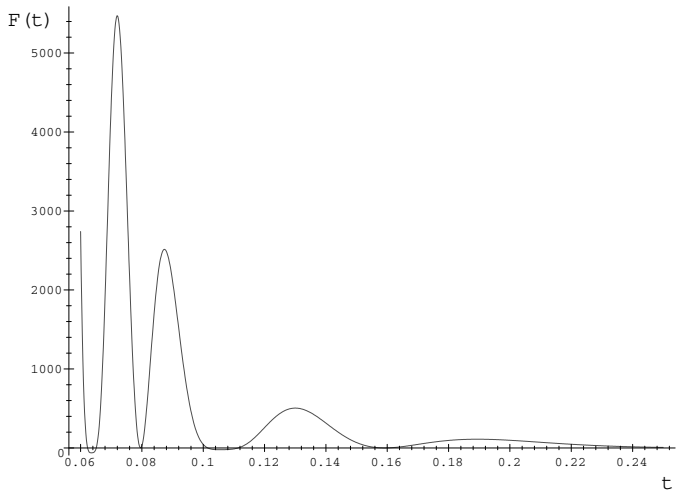

Figure 3. Graphical search for the roots of $F(t)$.

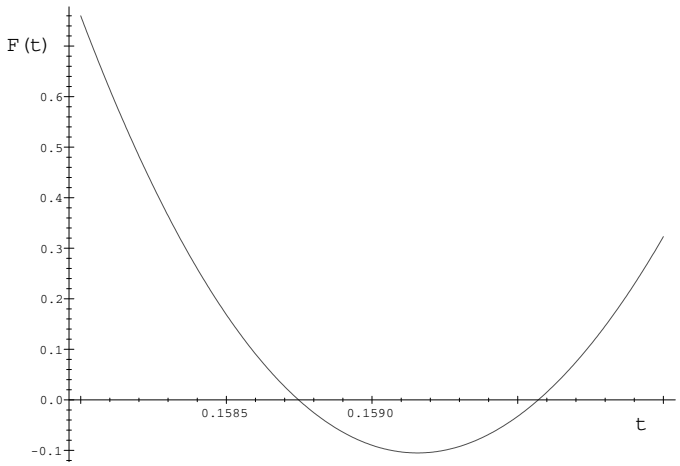

Figure 4. A magnification of figure 3 near $t = 0.16$.

The comparatively larger distance between t_{2k-1} and t_{2k} at odd $k = 2m + 1$ makes the numerical determination of these pairs less difficult. Conversely, the quick decrease of distance between these roots at even $k = 2m$ may be perceived, especially in combination with the growth of the maxima of $F(t)$ at the smaller $t \to 0$, as the key obstacle encountered during the precise numerical localization of the energies. A useful tool for the disentanglement of these two obstacles has been found in the introduction of an auxiliary function $L(t) = \log[|F(t)|]$, the practical *numerical* picture of which is sampled in figure 5.

Two of its properties have to be emphasized. Firstly, the absolute-value-part of the definition of $L(t)$ guarantees that the logarithm remains well defined *and* that the changes of sign of the original functions $F(t)$ on a very small interval become, empirically, 'magnified'. The emergence of every quasi-degenerate pair of zeros will be reflected by a very well visible 'artificial bump' in $L(t)$ in place of a hardly visible doublet of nodes in an improperly rescaled graph of the unmodified function $F(t)$ (compare, e.g., figures 4 and 5).

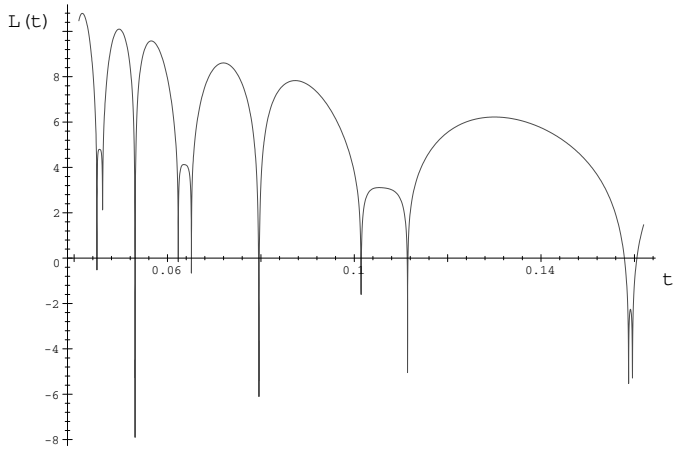

Figure 5. Logarithmic re-scaling $L(t) = \log[|F(t)|]$ and an improved graphical trapping of quasi-degeneracy.

Secondly, the sequence of the maxima of $L(t)$ will not grow that quickly with the decrease of $t \ll 1$. Hence, the growing density of the roots is better represented by the logarithm, in spite of its, in principle, unlimited decrease near the zeros of $F(t)$. Empirically, the latter effect proves negligible in numerical practice, in a way illustrated very persuasively by figure 5.

We may summarize that the main experience gained during the graphical solution of our sample secular equation (15) lies in the necessity of an appropriate selection of the interval in which the separate roots t_n are being sought. Of course, the 'good' size of these intervals will depend on the coupling Z so that, in general, one should never forget to consult the graphs of $F(t)$ *and* $L(t)$, which carry complementary information.

5. Discussion

5.1. Multiple-well problems in a non-Hermitian framework

We may summarize that a family of certain purely imaginary potentials was considered on a circle. Their piece-wise constant shape was chosen to mimic the multi-well angular part of certain not yet fully understood pseudo-Hermitian versions of Calogero–Moser and Smorodinsky–Winternitz Hamiltonians with real energies. Conversely, the reality of our spectrum reflects a 'minimal' square-well-type $\mathcal{PT}$ symmetrization of the initial many-body or more-dimensional separable Hamiltonian. A thorough numerical analysis of the spectrum was performed for the first non-trivial special case with double-well potential. It has been shown to exhibit a rich 'four series' structure.

These results fit well a broader perspective. Forty years ago, perturbation analysis of the single-well oscillator $H^{(\mathrm{SW})}(g) = p^2 + x^2 + g^2x^4$ revealed that the most natural interpretation of its 'physical' spectrum $\{\varepsilon_n(g)\}$ emerges via a complexification of its coupling g [31]. *All* the apparently uncorrelated numbers $\varepsilon_n(g)$ were shown to coincide with the values of a *single* analytic function $\varepsilon(g)$, evaluated on the *different* Riemannian sheets. In this interpretation, the main quantum number $n = 0, 1, \ldots$ merely selects the different Riemannian sheets in a certain specific, very transparent and intuitively appealing manner. One may conclude that the complexification of the parameters is one of the best ways towards an understanding of the

spectra, especially when they exhibit a strongly anharmonic double-well shape [32] since, in these cases, there may exist a close connection between the single and double wells mediated by Fourier transformation and analytic continuation [12].

A priori one might expect that the high degree of an internal symmetry of the superintegrable equations (which implies their separability and exact solvability in several systems of coordinates [21]) might mediate the facilitated technical feasibility and, hence, preference of their systematic $\mathcal{PT}$ symmetrization. For this reason, our present recipe might be re-read as a direct 'brute-force' introduction of a Hermiticity-breaking term. Such a modification of the superintegrable Schrödinger equations by an additional potential might offer a new insight into the problem of the reality of the spectra and, in particular, into the (sub)problem of the mechanisms of its possible (and, in principle, admissible and often quite easy) breakdown.

5.2. Summary and outlook

The relationship of the $\mathcal{PT}$ symmetry of the Hamiltonian to the reality of its spectrum was illustrated here via a few most elementary non-Hermitian solvable models in two dimensions. In similar examples, the choice of suitable $\mathcal{PT}$ symmetric anharmonic terms is usually dictated by the purely technical requirements of simplicity and solvability. In this sense, one encounters serious difficulties when moving to two and more dimensions since only the one-dimensional Schrödinger equations abound with solvable potentials. For a successful $\mathcal{PT}$ symmetric generalization of these models to more dimensions, the key contribution of our present short paper may be seen in its proposal and verification of a combination of the matching and analytic techniques. We showed that in spite of the violation of the superintegrability caused by our introduction of the step-like imaginary potentials, we were still able to study our models by the essentially non-numerical technique.

The angular potentials we considered were drastically simplified to a piece-wise constant purely imaginary field which manifestly destroys the Hermiticity of the Hamiltonian. Our extreme simplification of the generic situation offered a picture where the barriers become penetrable. This changes the boundary conditions to periodic ones [14]. The related analysis proved extremely illuminating and revealed the existence of new and hardly expected types of regularity in the spectrum. We may conclude that our choice of the schematic toy model (9) was fortunate, indeed.

- Qualitatively, the energies in the spectrum seem to be classified as lying in four separate series.
- The intrinsic double-well character of the model seems to be responsible for the emergence of the almost degenerate energy doublets.
- One encounters the quasi-degeneracy of the energies not only in the low energy domain but, quite unexpectedly, all over the energy scale.

There exist several open questions which remained unanswered. Firstly, a deeper understanding of many empirical observations is missing. The quadruple-series spectrum in table 1 as re-emphasized in tables 2 and 3 might motivate a continuing analysis of more-dimensional systems.

Secondly, there is no doubt that the structure of the spectrum in our present $\mathcal{PT}$ symmetric model is richer than in its Hermitian predecessors. Although all the intuitive and/or elementary interpretations of the 'angular-type' motion over the circle remain similar, one feels tempted to emphasize the differences. In this sense, one notices, first of all, that our present model re-confirms the idea and/or existence of certain 'quantum beats' as conjectured on the basis of a different model in [30].

Thirdly, one has to re-emphasize that in contrast to the quasi-degeneracy as observed in the Hermitian multiple wells, the present, $\mathcal{PT}$-symmetric analogue of this phenomenon is 'periodic' and transcends the standard limitation of the quasi-degeneracy to the mere low-lying spectrum.

Finally, we might re-open the discussion which was initiated in [14]. An ambiguity of a return to the Hermitian case has been revealed there, and interpreted as a transformation which gives rise to the unexpected emergence of some entirely new models. Of course, once we started here from a separation of a circle into some $2M$ quasi-independent sectors, a similar outcome might be expected in principle. Indeed, our example just deals with the parts (quadrants) of a bigger phase space. As long as this space was originally decomposed into a few invariant subspaces, its non-Hermitization might offer a recipe how one could open a tunnel through the originally fully impenetrable barriers.

Acknowledgment

The work was supported by GA AS in Prague, contract no A 1048302.

References

[1] Sotona M and Žofka J 1974 *Phys. Rev.* C **10** 2646
[2] Kalnins E G 1986 *Separation of Variables for Riemannian Spaces of Constant Curvature* (Harlow: Longman)
[3] Friš J, Mandrosov V, Smorodinsky Ya A, Uhlíř M and Winternitz P 1965 *Phys. Lett.* A **16** 354
Evans N W 1991 *J. Math. Phys.* **32** 3369
Grosche C, Pogosyan G S and Sissakian A N 1995 *Fortsch. Phys.* **43** 453
[4] Calogero F 1969 *J. Math. Phys.* **10** 2191
[5] Turbiner A 1998 *Mod. Phys. Lett.* A **13** 1473
[6] Bender C M and Boettcher S 1998 *Phys. Rev. Lett.* **24** 5243
[7] Kowalski K and Rembelinski J 2002 *J. Phys. A: Math. Gen.* **35** 1405
Trifonov D A 2003 *J. Phys. A: Math. Gen.* **36** 2197
Nagasawa T, Sakamoto M and Takenaga K 2002 SUSY in QM with point interactions *Preprint* LANL hep-th/0212192
[8] Znojil M and Tater M 2001 *J. Phys. A: Math. Gen.* **34** 1793
[9] Pöschl G and Teller E 1933 *Z. Phys.* **83** 143
Lévai G and Znojil M 2001 *Mod. Phys. Lett.* A **16** 1973
Jia C-S, Sun Y and Li Y 2002 *Phys. Lett.* A **305** 231
[10] Fernández F M, Guardiola R, Ros J and Znojil M 1998 *J. Phys. A: Math. Gen.* **31** 10105
Bender C M, Cooper F, Meisinger P N and Savage V M 1999 *Phys. Lett.* A **259** 224
Znojil M 1999 *J. Phys. A: Math. Gen.* **32** 7419
Ahmed Z 2001 *Phys. Lett.* A **282** 343
Ahmed Z 2001 *Phys. Lett.* A **286** 231
Bagchi B, Quesne C and Znojil M 2001 *Mod. Phys. Lett.* **16** 2047
Bender C M, Berry M, Meisinger P N, Savage V M and Simsek M 2001 *J. Phys. A: Math. Gen.* **34** L31
Bagchi B and Quesne C 2002 *Phys. Lett.* A **300** 18
Lévai G, Cannata F and Ventura A 2002 *J. Phys. A: Math. Gen.* **35** 5041
Bagchi B, Mallik S and Quesne C 2002 *Int. J. Mod. Phys.* A **17** 51
[11] Feshbach H and Villars F 1958 *Rev. Mod. Phys.* **30** 24
[12] Buslaev V and Grechi V 1993 *J. Phys. A: Math. Gen.* **26** 5541
[13] Pontrjagin L S 1944 *Izv. Akad. Nauk SSSR Ser. Mat.* **8** 243
Gohberg I, Lancaster P and Rodman L 1983 *Matrices and Indefinite Scalar Products* (Basel: Birkhauser)
Scholtz F G, Geyer H B and Hahne F J W 1992 *Ann. Phys., NY* **213** 74
Mostafazadeh A 2002 *J. Math. Phys.* **43** 205, 2814, 3944 and 6343
[14] Znojil M and Tater M 2001 *Phys. Lett.* A **284** 225
[15] Hatano N and Nelson D R 1996 *Phys. Rev. Lett.* **77** 570
Feinberg J and Zee A 1999 *Phys. Rev.* E **59** 6433

Shnerb N M 2001 *Phys. Rev.* E **63** 011906
Klishevich S M and Plyushchay M S 2001 *Nucl. Phys.* B **606** 583
Scolarici G and Solombrino L 2002 *Phys. Lett.* **303** 239
Weigert S 2002 *Preprint* LANL quant-ph/0209054
Ramírez A and Mielnik B 2002 *Preprint* LANL quant-ph/0211048 (2003 *Rev. Fis. Mex.* at press)
[16] Bender C M and Milton K A 1997 *Phys. Rev.* D **55** R3255
Bender C M, Boettcher S and Meisinger P N 1999 *J. Math. Phys.* **40** 2201
[17] Caliceti E, Graffi S and Maioli M 1980 *Commun. Math. Phys.* **75** 51
[18] Alvarez G 1995 *J. Phys. A: Math. Gen.* **27** 4589
Delabaere E and Pham F 1998 *Phys. Lett.* A **250** 25
Delabaere E and Trinh D T 2000 *J. Phys. A: Math. Gen.* **33** 8771
Mezincescu G A 2000 *J. Phys. A: Math. Gen.* **33** 4911
Handy C R, Khan D, Wamg Xiao-Xian and Tomczak C J 2001 *J. Phys. A: Math. Gen.* **34** 5593
Dorey P, Dunning C and Tateo R 2001 *J. Phys. A: Math. Gen.* **34** 5679 and L391
[19] Bender C M and Boettcher S 1998 *J. Phys. A: Math. Gen.* **31** L273
Znojil M 2000 *J. Phys. A: Math. Gen.* **33** 4203
[20] Bender C M, Dunne G V, Meisinger P N and Simsek M 2001 *Phys. Lett.* A **281** 311
Nanayakkara A and Abayaratne C 2002 *Phys. Lett.* A **303** 243
[21] Tempesta P, Turbiner A V and Winternitz P 2001 *J. Math. Phys.* **42** 4248
[22] Calogero F 1971 *J. Math. Phys.* **12** 419
Olshanetsky M A and Perelomov A M 1983 *Phys. Rep.* **94** 313
Rühl W and Turbiner A 1995 *Mod. Phys. Lett.* A **10** 2213
[23] Znojil M 2001 *Phys. Lett.* A **285** 7
Znojil M and Lévai G 2001 *Mod. Phys. Lett.* A **16** 2273
Albeverio S, Fei S M and Kurasov P 2002 *Lett. Math. Phys.* **59** 227
Deb R N, Khare A and Roy B D 2003 *Phys. Lett.* A **307** 215
Korsch H J and Mosman S 2003 *J. Phys. A: Math. Gen.* **36** 2139
[24] Basu-Mallick B and Mandal B P 2001 *Phys. Lett.* A **284** 231
[25] Jakubský V and Znojil M 2003 Complex Smorodinsky–Winternitz models with real energies in preparation
[26] Znojil M 2001 *J. Phys. A: Math. Gen.* **34** 9585
[27] Cannata F, Junker G and Trost J 1998 *Phys. Lett.* A **246** 219
[28] Bender C M, Dunne G V and Meisinger P N 1999 *Phys. Lett.* A **252** 272
[29] Jones H J 1999 *Phys. Lett.* A **262** 242
[30] Znojil M 2003 Solvable simulation of a double-well problem in PT symmetric quantum mechanics *Preprint* LANL quant-ph/0303122 (*J. Phys. A: Math. Gen.* at press)
[31] Bender C M and Wu T T 1969 *Phys. Rev.* **184** 1231
Turbiner A V and Ushveridze A G 1988 *J. Math. Phys.* **29** 2953
[32] Flessas G P and Watt A 1981 *J. Phys. A: Math. Gen.* **14** L315
Avron J and Seiler R 1981 *Phys. Rev.* D **23** 1316
Burrows B L, Cohen M and Feldman T 1989 *J. Phys. A: Math. Gen.* **22** 1303
Znojil M 1997 *J. Math. Phys.* **38** 5087